Bioengineer mesenchymal stem cell for Treatment of glioma by IL-12 mediated microenvironment reprogramming and nCD47-SLAMF7 mediated phagocytosis regulation of macrophages

Man Li[1,2*], Lisen Lu[3*], Qungen Xiao[2], ALI ABDI MAALIM[2], Bin Nie[1], Yanchao Liu[2], Kai Shu[2], Ting Lei[2], Mingxin Zhu[2]

1.Department of Anesthesiology and Pain Medicine, Hubei Key Laboratory of Geriatric Anesthesia and Perioperative Brain Health, and Wuhan Clinical Research Center for Geriatric Anesthesia, Tongji Hospital, Tongji Medical College, Huazhong University of Science and Technology.

2.Department of Neurosurgery, Tongji Hospital, Tongji Medical College, Huazhong University of Science and Technology, Wuhan, People's Republic of China

3.College of Biomedicine and Health and College of Life Science and Technology, Huazhong Agricultural University, Wuhan, 430070, China.

* Man Li and Lisen Lu contributed equally to this work.

Corresponding Author:

Mingxin Zhu, Department of Neurosurgery, Tongji Hospital, Tongji Medical College, Huazhong University of Science and Technology, Wuhan, Hubei, People's Republic of China. Email: mxzhu@tjh.tjmu.edu.cn

Abstract:

High expression of cellular self-activated immunosuppressive molecules and extensive infiltration of suppressive immune cells in the tumor microenvironment are the main factors leading to the resistance of glioma to immunotherapy. However, the technology related to modifying the expression of glioma cellular self-molecules based on gene editing still needs to be developed. In this project, cell therapy strategies were developed to reverse the immunosuppressive microenvironment of glioma (TIME). Mesenchymal stem cells (MSCs) derived from bone marrow were used as carriers to express bioactive proteins, which could exhibit tumor-homing characteristics in response to tumor TGF-β signals. MSCs were modified to express the secretory anti-tumor immune cytokine IL-12 and the nCD47-SLAMF7 fusion protein, which regulates the phagocytosis of macrophages. The engineered MSCs are then injected in situ into the area near the glioma to bypass the blood-brain barrier and provide localized high concentrations of bioactive proteins. This approach could significantly activate natural and adaptive immune cells in the TIME, ultimately leading to the effective control of glioma. This study provides a new strategy for the clinical treatment of glioma patients and the prevention of postoperative recurrence.

Introduction:

Glioma is the most common primary tumor of the central nervous system[1]. The tumor's unique location and its invasive growth characteristics make complete removal of glioma challenging. Furthermore, the existence of the blood-brain barrier and the interaction between neurons and the tumor limit the effect of clinical radiotherapy and chemotherapy[2]. Consequently, the average survival time of glioma patients is only 14 months. In recent years, immune checkpoint blocking (ICB) has achieved a breakthrough and has been successfully used in the treatment of many types of tumors, but its therapeutic effect on glioma is not ideal[3]. The main reason is the immunosuppressive microenvironment caused by the massive infiltration of MDSC, the promotion of tumor TAM differentiation, and the abnormal proliferation of blood vessels[4].

The factors contributing to glioma's resistance to immunotherapy include both endogenous and exogenous elements. Endogenous factors involve the activation of the β-catenin signaling pathway[5], high expression of PD-L1[6], and high expression of immune inhibitory molecules, such as IDO[7] and PEG2[8]. However, there are significant technical challenges in modifying the gene expression profile of glioma cells in vivo. Exogenous factors include the infiltration of various immunosuppressive cells and the expression of related inhibitory molecules[9, 10], while macrophages constitute more than half of the immune cells infiltrating glioma, secreting immunosuppressive molecules like IL-4, IL-10, and SIRRα[11]. These molecules can effectively enable glioma cells to evade innate immune recognition, thus limiting the efficacy of adaptive immune responses. Moreover, the interaction between CD47 and SIRPα has been recognized as a classical immunosuppressive signaling pathway[12]. Radiotherapy has been found to increase the expression of CD47 in glioma patients by altering mitochondrial fatty acid oxidation levels[13]. The trans-interactions of the CD47/SIRPα axis and cis-interaction of CD47/SLAMF7 (member of the signaling lymphocyte activating molecule family 7) inhibits phagocytosis and antigen

presentation by phagocyte-like cells to tumor cells, which in turn inhibits the killing effect of innate immune cells on tumor cells and further inhibits direct recognition by adaptive immune cells[14]. However, since CD47 is also expressed by blood cells and other normal cells, the use of anti-CD47 antibody therapy is limited in its effectiveness[15]. As an important indicator of the regulation of tumor phagocytosis by phagocytic cells, SLAMF7 has been employed in the treatment of triple-negative breast cancer using a bispecific nanobioconjugate, demonstrating promising efficacy[16]. Therefore, developing a strategy to locally modulate CD47 activity and inhibit its interaction with SLAMF7 could effectively counteract the contribution of exogenous factors to immunotherapy resistance in glioblastoma multiforme (GBM).

Cell therapy plays a crucial role in anti-tumor immunity, including CAR-T cells, TCR-T cells, CAR-macrophages, and CAR-NK cells, all of which have demonstrated tumor-killing efficacy[17-20], However, its application is limited due to MHC restriction, tumor cell heterogeneity, and the presence of an immune-regulatory microenvironment[21, 22]. Mesenchymal stem cells (MSCs) are a group of cells characterized by a low degree of differentiation, strong proliferative capacity, high differentiation potential, and a unique ability to "home" to tumors[23, 24]. MSCs have been used for preclinical GBM therapy in a variety of forms, including MSCs themselves[25], MSC-derived extracellular vesicles[26], oncolytic virus vectors[27], suicide protein expression containers[28], and immune-activating cytokine vectors[29]. Previous work in this study developed a promoter system that is responsive to TGF-β, using the properties of MSCs to react to this cytokine. This system specifically enhanced the expression of relevant cytokines by MSCs within the GBM microenvironment, which is rich in TGF-β. This, in turn, significantly inhibited the growth of a mouse glioma model.[30]. This project continues to capitalize on the advantages of MSCs in anti-tumor immunotherapy and achieves the reversal of the glioma immunosuppressive microenvironment (TIME) through genetic programming, effectively inhibiting the in vivo growth of GL261 tumor cells.

As IL-12 cytokines have been reported to enhance natural and cellular immune effects in a variety of tumors[31, 32], MSCs were designed to express IL-12 cytokines

and nCD47-SLAMF7 fusion protein under the control of TGF-β concentration. NCD47-SLAMF7 consists of a signaling peptide, a nanobody that can block the function of CD47, and the extracellular region of SLAMF7, which can target tumor cells and mask their CD47 molecules. This allows tumor cells to present SLAMF7 on their surface. The strategy facilitates the uptake of tumor cells by SLAMF7-expressing macrophages and activates innate and cellular immunity in glioma, thereby effectively controlling the progression of the disease. In this study, we found that the levels of IL-12 and SLAMF7 expressed by clinical tumor patients were not sufficient to regulate the tumor immunosuppressive microenvironment (TIME), as determined through analysis of clinical databases and the Human Protein Atlas. Furthermore, the CD47/SIRPα axis expression in the mouse glioma model was consistent with that in clinical patients. Genetically engineered MSCs, with their homing properties, have been demonstrated to effectively release IL-12 cytokines and the nCD47-SLAMF7 fusion protein by activating the Smad4 transcription factor in a TGF-β-rich environment. Additionally, supernatants from MSCs expressing these proteins were found to effectively promote T cell proliferation and activation, as well as enhance the phagocytic and antigen-presenting abilities of macrophages against tumor cells. The results of in vitro and in vivo experiments demonstrated that MSCs expressing the aforementioned proteins could effectively home to tumor sites. These MSCs were shown to promote macrophage-mediated phagocytosis of tumor cells and the activation of effector T cells, as well as the in vivo release of cytokines associated with anti-tumor immunity. Consequently, this led to the effective containment of glioma model development and provides a new therapeutic strategy for the treatment of patients with glioblastoma multiforme (GBM).

Results：

1. Clinical correlation between different functional proteins and glioma patients

By analyzing relevant functional proteins in TCGA_GBM patients with survival software and survminer software, we found that IL-12, SIRPα, CD47, and SLAMF7 did not show a significant association with clinical prognosis (Fig. 1A-D). However, the expression levels of IL-12, CD47, and SLAMF7 were higher in tumors than in adjacent non-tumorous tissues (Fig. 1E), as determined by analyzing their mRNA expression levels in glioma patients using TCGA and GTEx datasets. Furthermore, their expression was strongly correlated with immune cell infiltration (Fig. 1F, with the related analysis method described in the Methods section). Preclinical studies demonstrated a significant correlation between the regulated expression of these proteins and the survival of a mouse tumor model. Additionally, data from the Human Protein Atlas database indicated that IL-12 expression in glioma was much lower than in melanoma (Fig. 1G), suggesting that the levels of these proteins in glioma patients might be insufficient to modulate changes in the TIME.

To investigate whether the expression of SIRPα, CD47, and SLAMF7 in the mouse glioma model is consistent with that in clinical patients, this study established an in-situ glioma model using GL261 cells. Immunofluorescence analysis of tumor sections showed that SLAMF7 was mainly localized to the tumor periphery, with lower levels in the tumor core (Fig. 1H), implying that SLAMF7 expression may hinder glioma development. Moreover, despite the large infiltration of macrophages and microglia secreting abundant SIRPα, CD47 molecules were also highly expressed and colocalized with SIRPα in the TIME (Fig. 1I), illustrating a typical immunosuppressive interaction between SIRPα and CD47 molecules. Overall, these findings confirm that the GL261 glioma model has a protein expression profile similar to that of clinical patients.

2.Controllable expression, structural accuracy and targeting of immune cells for IL-12 and nCD47-SLAMF7 expressed in MSC.

The side effects of drugs, the presence of the blood-brain barrier, and the limited concentration of drugs in the tumor microenvironment limit the clinical efficacy of glioma treatment. To overcome these challenges, engineered MSCs with tumor-homing and TIME-responsive properties were developed. These cells are driven by transcription factors such as SMAD4 to release IL-12 or nCD47-SLAMF7 fusion proteins for glioma cell therapy. SMAD4 is an effector downstream of the TGF-β receptor and can respond with high sensitivity to TGF-β and other cytokines in the tumor microenvironment (Figure 2A-B). The nCD47-SLAMF7 construct includes a signal peptide sequence, a nanobody that targets to shield the function of CD47, a linker containing (GGGSGGGG)2, and the SLAMF7 extracellular structural domain $SLAMF7_{23\text{-}224}$. To characterize the controlled expression of IL-12 and nCD47-SLAMF7 in MSCs, the mCherry protein was fused to the C-terminus of the target proteins. The results in Figure 2C-D showed that adding TGF-β cytokine to the culture medium could effectively induce the expression of IL-12 and nCD47-SLAMF7. The culture medium (CM) of MSC-IL-12 or MSC-nCD47-SLAMF7 was collected and used for non-denaturing SDS-PAGE experiments after incubating with TGF-β for 24 hours. Figure 2E showed that the molecular weights of IL-12 and nCD47-SLAMF7 secreted into the MSC-CM were approximately 70 kDa and 50 kDa, respectively, consistent with the designed proteins. The ELISA results (Figure 2G and 2I) confirmed that the supernatant secreted by the MSCs contained high levels of IL-12 or nCD47-SLAMF7. Immunoblotting experiments confirmed the sequence accuracy of these proteins (Figure 2F and 2H).

To verify that IL-12 or nCD47-SLAMF7 secreted into the CM could effectively target downstream cells, spleen-derived CD8 T cells (Figure 2K) with a high expression of the IL-12 receptor and GL261 cells with high expression of CD47 molecules (Figure 2M) were used as targets. Confocal imaging results (Figure 2J) showed that IL-12-mCherry could effectively bind to the membranes of CD8+ T cells when incubated with the MSC-IL-12-mCherry culture medium, while nCD47-SLAMF7-mCherry could also effectively bind to the membranes of GL261 cells when incubated with the supernatant of MSC-nCD47-SLAMF7-mCherry cells.

Figures 2L and 2N further supported the conclusion regarding the targeting ability of IL-12 and nCD47-SLAMF7, as demonstrated by flow cytometry.

3. Characterizing the functional effects of IL-12 or nCD47-SLAMF7 contained in MSC culture medium on CD8 T cells or macrophages.

The main purpose of using MSCs to express IL-12 and nCD47-SLAMF7 in this study was to achieve controlled release in the tumor microenvironment as well as effective reversal of the TIME, thus activating both natural and adaptive immunity for effective treatment of glioma. To verify the functional effects of IL-12 and nCD47-SLAMF7 on downstream immune cells, we chose OT-I T cells, which specifically recognize OVA antigens, and bone marrow-derived macrophages as the subjects of the study. The OT-I $CD8^+$ T cells obtained by magnetic bead sorting were labeled with CFSE dye and then co-incubated with GL261-CM or MSC-CM containing IL-12 for 48 hours followed by the detection of OT-I T cell proliferation and the expression of IFN-γ. **Figure 3A-B** showed that IL-12-containing MSC-CM efficiently induced more T cell proliferation and the production of the effector molecule IFN-γ compared to GL261-CM. Furthermore, bone marrow-derived undifferentiated M0 macrophages were co-incubated with GL261-CM or MSC-IL-12-CM for 24 h, and the classical M1-type marker CD86 and the classical M2-type marker CD206 was used to label the macrophages. **Figure 3C-D** showed that GBM-CM induced high expression of CD206 in M0-type macrophages and had no effect on the expression of CD86, indicating that they were polarized toward M2-type macrophages. In contrast, M0-type macrophages incubated with MSC-IL12-CM expressed high levels of CD86 and did not promote the expression of CD206, indicating polarization toward M1-type macrophages. These results demonstrated that IL-12 produced by MSC can regulate the development of innate immune cells and adaptive immune cells towards anti-tumor immunity.

CD47-SIRPα interactions are well-established targets in natural immunomodulation, but the systemic toxicity of CD47 antibodies has limited their clinical application. Strategies that allow for the controlled release of CD47 antibodies

responsive to the tumor microenvironment have reduced this systemic toxicity. In this study, a CD47 antagonistic nanobody[33] was utilized to bind the extracellular region of SLAMF7 molecules, which can modulate the phagocytic activity of phagocyte-like cells, and the relevant regulatory mechanism is illustrated in **Figure 3E**. To observe the phenomenon of tumor cell phagocytosis by M0-type macrophages incubated with MSC-nCD47-SLAMF7-CM, GL261 tumor cells were labeled with PKH67, and M0 macrophages were labeled with PKH26 dyes, respectively. Subsequently, the two cell types were co-cultured with the addition of MSC-nCD47-SLAMF7-CM. **Figure 3F** shows that the macrophages could efficiently phagocytose tumor cells in the medium containing nCD47-SLAMF7, In contrast, neither MSC-IL12-CM nor GL261-CM enhanced the macrophages' phagocytic activity (**Figure 3G**). Additionally, the culture medium containing both IL-12 and nCD47-SLAMF7 had a more pronounced effect on promoting macrophage phagocytosis, which may be due to IL-12 influencing the polarization state of macrophages.

To establish that macrophages can initiate the adaptive immune system after uptake of tumor cells, OVA-expressing GL261 cells with knockdown of the β2m gene (GL261-OVA$^{\beta 2m-/-}$) were generated by virus transduction. This cell line does not express MHC-I proteins and cannot present OVA class I antigens on the cell surface, thus preventing the stimulation and proliferation of OT-I T cells by the tumor cells themselves. We combined the macrophages and GL261-OVA$^{\beta 2m-/-}$ tumor cells in a mixed system with GL261-CM or MSC-nCD47-SLAMF7-CM for 24 hours and then co-incubated with OT-1 T cells labeled with CFSE. The proliferation of OT-1 T cells and the release of inflammatory factors such as IFN-γ after 48 hours was examined. **Figure 3H-I** showed that macrophages that had phagocytosed GL261-OVA$^{\beta 2m-/-}$ tumor cells efficiently induced the proliferation of OT-I T cells and the significant release of the effector molecule IFN-γ. However, macrophages that phagocytosed tumor cells less efficiently did not produce this effect. These results confirm that nCD47-SLAMF7 enhances the phagocytic activity of phagocyte-like cells on tumors and initiates adaptive immune responses.

4. Identify the tumor-homing ability of MSC-IL-12 or MSC-nCD47-SLAMF7.

The choice of MSC as a carrier for cell therapy strategy in this study lies in the fact that MSC has natural tumor-homing properties. To ascertain whether overexpression of IL12 or nCD47-SLAMF7 affects the homing properties of MSCs, a personalized transwell model was designed, and the relevant schematic diagrams are shown in **Figure 4A**. The surface area was inoculated with MSC expressing the EGFP fluorescent protein, while the left and right compartments were filled with astrocyte-CM and GL261-CM, respectively. **Figure 4B** showed that MSC expressing either IL12 or nCD47-SLAMF7 have the potential for convergent movement toward the GL261-CM. To determine whether TGFβ in the GL261-CM induced the chemotactic movement of MSC, a TGF-β receptor inhibitor (LY2109761, 10 ng/mL) was added to the GL261-CM. H&E staining of the transwell (**Figure 4C**) demonstrated that GL261-CM efficiently promoted the infiltration of MSCs, whereas GL261-CM containing LY2109761 blocked this function, indicating that TGF-β released by GL261 is the main cytokine-inducing MSC homing.

To validate the in vivo tumor-homing effect of MSCs expressing IL-12 or nCD47-SLAMF7, we constructed astrocyte and GL261 tumor cell lines expressing mCherry, as well as MSCs expressing IL12-EGFP and nCD47-SLAMF7-EGFP. The schematic diagrams of the injection strategy are shown in Figure 4D. Seven days after in situ injection, the mice's brains were subjected to immunofluorescence staining. Confocal imaging (Figure 4E) revealed that the number of IL-12-expressing MSCs homing toward the astrocyte population was minimal, while a relatively large number of cells homed toward the GL261 cell population. MSCs expressing nCD47-SLAMF7 did not affect the homing ability of the MSCs.

5. In vivo validation of MSC-IL-12 and MSC-nCD47-SLAMF7 for glioma treatment.

The previous results confirmed that the engineered MSCs had been successfully constructed and could effectively be home to glioma sites. To determine whether this cell therapy strategy could control the growth of in situ glioma in vivo, we used GL261-luciferase (GL261-Luc) cells to establish a mouse glioma model, with the treatment protocol outlined in Figure 5A. Different groups of mice were imaged using

in vivo small animal imaging, and the intensity of bioluminescence was measured at various time points. Figure 5B showed that a single injection of MSCs expressing either IL-12 or nCD47-SLAMF7, as well as a mixed injection of both types of cells on day 6, could inhibit glioma growth to some extent. Most importantly, the group injected with a combination of the two cell types exhibited the most significant inhibition of glioma growth. The statistics of bioluminescence intensity on day 0 (**Figure 5C**) and day 16 (**Figure 5D**) indicated that MSCs expressing both target proteins imposed a stronger inhibitory effect on GBM growth. Survival analysis (Figure 5E) revealed that MSCs expressing either IL-12 alone or nCD47-SLAMF7 alone could improve the survival rate of the mouse model to a certain extent. However, the combined anti-tumor treatment effect of the two significantly enhanced the survival rate of the mice.

To confirm whether the injected MSCs had effects localized to the tumor and to monitor tumor growth in vivo, GL261-mCherry cells were injected on day 0. Different groups of EGFP-expressing MSCs were then injected on day 6. On day 16, immunofluorescence experiments were conducted on the mice to observe the co-localization of GL261 cells with MSCs. Figure 5F showed that the GL261 cell population was the smallest in the group injected with a mixture of MSCs, while there was a high degree of co-localization between MSCs and GL261 cells in different groups. These phenomena proved that MSCs primarily acted within the tumor in situ. We also observed the effects on immune cells in the TIME after injection with different groups of MSCs.

The colocalization results in Figure 5G showed that both normal GL261 tumors and those injected with the normal MSC group contained a large number of M2-type macrophages (macrophages in green, CD206 signals in red). In contrast, the number of M2-type macrophages was low in both the MSC-IL-12 injection group and the mixed MSC injection group. This indicated that cytokines such as IL-12 could alter the differentiation status of macrophages. This finding is consistent with the in vitro results of inducing differentiation of M0-type macrophages toward the M1-type. However, the injection of MSC-nCD47-SLAMF7 did not significantly reduce the

differentiation of M2-type macrophages, a result also supported by the statistical data in Figure 6A. The observations in Figure 5H, along with the statistical data in Figure 6C, demonstrated that injections of MSC groups expressing IL-12 or nCD47-SLAMF7 led to a substantial increase in CD8 T-cell infiltration compared to the normal MSC group, with the mixed MSC group exhibiting the highest level of CD8 T-cell infiltration. These results confirmed that the combination of IL-12 and nCD47-SLAMF7 could effectively modulate the tumor-suppressive microenvironment and promote extensive infiltration of anti-tumor effector T cells, thereby effectively inhibiting glioma progression.

6. Validation of the ability of MSC-IL-12 and MSC-nCD47-SLAMF7 to reverse the TIME

Injections of mixed MSCs expressing different target proteins have effectively inhibited the growth of GL261 in situ and significantly influenced macrophage differentiation and CD8 T-cell infiltration. We also investigated their impact on DC cells, functional T-cells, and precursor exhausted-like T-cells (a subset exerting a predominantly anti-tumor effect). Flow cytometry results indicated that the mixed injection of MSCs expressing both IL-12 and nCD47-SLAMF7 led to a marked increase in DC cell maturation and activation within the TIME (Figure 6B), induced more effector $CD8^+$ T-cells to release pro-inflammatory cytokines like IFN-γ (Figure 6D), and enhanced the infiltration of $TCF\text{-}1^+$ T-cells (Figure 6E), thereby generating a more sustained anti-tumor immune response..

To observe nCD47-SLAMF7-induced phagocytosis of tumor cells by macrophages in vivo, immunofluorescence was performed on glioma models injected with MSC-IL-12 or MSC-nCD47-SLAMF7.**Figure 6F** showed that macrophages in the MSC-nCD47-SLAMF7-injected group (green fluorescent markers) effectively encapsulated GL261 tumor cells (red fluorescent markers), while macrophages in the MSC-IL-12-injected group did not actively ingest tumor cells.

To further substantiate the impact of mixed MSCs on the TIME, we also examined the expression of cytokines associated with anti-tumor immunity using a custom multi-cytokine assay kit. Figures 6G-N demonstrated that, compared to other

groups, pro-inflammatory cytokines such as TNF-α and IL-6 were significantly upregulated in the supernatant from the glioma mouse model injected with the mixed MSC group. Additionally, IFN-γ (associated with CD8 T-cell activity) and CXCL9 and CXCL10 (associated with T-cell infiltration) were also markedly elevated, with some increase observed in the MSC-IL-12 and MSC-nCD47-SLAMF7 groups compared to the control MSC group. Furthermore, cytokines related to macrophage infiltration and differentiation, such as GM-CSF, CCL2, and IL-12, were significantly upregulated in the supernatant from both the single MSC injection groups and the mixed injection group, with the latter showing higher levels. These results confirm that a strategic combination of active proteins with MSCs plays a crucial role in modulating the TIME and offers a novel therapeutic approach for the clinical treatment of GBM patients.

Discussion

In this study, MSCs were used as carriers for a cell therapy strategy, utilizing their tumor-homing characteristics that respond to TGFβ to achieve controlled release of bioactive proteins (IL-12 or nCD47-SLAMF7) in the tumor microenvironment while avoiding systemic toxicity. By fully activating both innate and adaptive immune cells, the strategy effectively reversed the TIME and delayed the progression of glioma. Overall, this study proposes a novel therapeutic approach for the clinical treatment of GBM patients.

The CD47/SIRPα signaling axis plays a crucial role in promoting the formation of the TIME, wherein CD47 can cis-bind to the pro-phagocytosis protein SLAMF7, inhibiting its dependent phagocytosis effects, in addition to trans-binding to SIRPα[14]. Furthermore, CD47 monoclonal antibody-mediated phagocytosis requires the SLAMF7 signaling pathway[34], as studies have shown that SIRPα expression in macrophages reduces CCL8 secretion by inhibiting Syk/Btk kinase activity, thereby impeding T cell recruitment and subsequent anti-tumor responses[35]. These studies revealed that pairing the CD47 antibody with SLAMF7 might enhance tumor phagocytosis of macrophages rather than combining the SIRPα antibody with SLAMF7. In this study, we opted to use nanobodies instead of traditional antibodies

primarily because nanobodies lack the Fc segment, which can effectively reduce the risk of Fc receptor-mediated inflammatory diseases[36], and their shorter amino acid sequences and simple post-translational modifications can promote their massive expression in target cells.

The full-length SLAMF7 protein and CD47 nanobody were initially designed to construct a fusion protein targeting tumor cells. However, the fusion protein could not be transported into the supernatant via the exocytosis signal peptide sequence. The primary reason may be that the α-helix structure formed by $SLAMF7_{225-245}$ in the SLAMF7 protein prevents its exocytosis into the MSC supernatant. To enhance the secretion of the nCD47-SLAMF7 fusion protein, this study utilized $SLAMF7_{23-224}$ (the extracellular domain of SLAMF7) to bind to the anti-CD47 nanobody and added signal peptide sequence to its N-terminal. Figure 2I demonstrates that the use of truncated SLAMF7 can effectively promote the exocytosis of fusion proteins while preserving their ability to modulate tumor phagocytosis by macrophages. This is the first time the use of truncated $SLMAF7_{23-224}$ has been proposed as a substitute for the function of full-length SLAMF7 in exerting biological effects.

The disadvantages of cell therapy strategies such as CAR-T or CAR-NK include off-target effects and cytokine storms caused by uncontrolled cell expansion. However, the MSCs used in this study are programmed to undergo apoptosis or differentiate locally into other cell types after 10 generations of propagation, which does not lead to severe cytokine storms (data not shown). Moreover, using MSCs as carriers for cell therapy enables the local delivery of high concentrations of biofunctional proteins and overcomes the blood-brain barrier through in situ injections, providing a novel therapeutic strategy for the clinical treatment of GBM patients or for preventing the recurrence of GBM after surgery.

Methods

Mice

C57BL/6 female mice were obtained from Hunan Slyke Jingda Laboratory Animal Co. Ltd. in Hunan, China. These mice were bred and maintained in a specific pathogen-free (SPF) barrier facility. All animal studies were conducted under the approval of the Hubei Provincial Animal Care and Use Committee and followed the experimental guidelines established by the Animal Experimentation Ethics Committee of Huazhong University of Science and Technology. This study was approved by the Ethics Committee of Huazhong University of Science & Technology (IRB ID:TJ20170201).

Cell lines

The murine glioma cell line GL261 was purchased from the National Cancer Institute (NCI, Frederick, MD, USA) and cultured in DMEM low glucose (Sigma-Aldrich, St. Louis, Missouri, USA) supplemented with 10% (v/v) fetal bovine serum (FBS Superior, Sigma-Aldrich), 1% (v/v) MEM non-essential amino acid solution (Thermo Fisher Scientific, Waltham, MA, USA), and 1% (v/v) penicillin/streptomycin (Sigma-Aldrich). Mouse astrocytes were obtained from the China Center for Type Culture Collection (Wuhan, China) and grown in Dulbecco's Modified Eagle's Medium (DMEM) (Gibco, Grand Island, NY, USA) containing 10% Fetal Bovine Serum (FBS) (Gibco, Grand Island, NY, USA) and 1% penicillin/streptomycin solution.. Mouse bone marrow-derived macrophages (BMDMs) were generated as previously described[37]. Murine MSCs were purchased from Pro-cell (Cat number # CP-M131) and cultured in Complete medium (specifically designed for mouse MSCs, purchased from Pro-cell) containing 10% (v/v) FBS and 1% (v/v) penicillin/streptomycin. Selection of murine MSC-IL-12 or MSC-nCD47-SLAMF7 was maintained with 100 pg/ml G418 (Sigma-Aldrich). Preparation of MSC for injection into mice was performed as described[30]. All cells were maintained in an incubator at 37 ℃ in a humidified atmosphere of 95% and 5% CO_2. The cell lines were examined for mycoplasma and viruses according to the FELASA guidelines by

Charles River Research Animal Diagnostic Services (CR RADS.Wilmington, MA, USA: Mouse essential panel) before in vivo transplantation.

Analysis of the relationship between functional proteins and immune cell infiltration

The ssgsea algorithm in R package "GSVA" was utilizedto quantify the immune cell infiltration of different cancers. The Marker gene set of immune cells came from the reference article “Pan-cancer Immunogenomic Analyses Reveal Genotype Immunophenotype Relationships and Predictors of Response to Checkpoint Blockade”. The relationship between the expression of IL12A, CD47, SIRPα and SLAMF7 mRNA and 28 immune cell subsets was studied by using R software package "pheatmap", and the heat map was generated by Spearman correlation analysis.

Lentiviral production, infection, and identification

GL261-OVA$^{\beta 2m-/-}$ was transduced with lentiviral vectors coding for OVA and sh RNA for β2m. Astrocyte-mCherry cells were transduced with lentiviral vectors coding for mCherry. For both in vitro and in vivo experiments, mouse MSCs were transduced with lentiviral vectors encoding EGFP, EGFP/Fluc, mCherry, or mCherry/Fluc, as well as lentiviral vectors driving the expression of IL-12 (peptide sequence shown in Supplementary Table) or nCD47-SLAMF7 (peptide sequence shown in Supplementary Table) in response to TGF-β[30]. To confirm TGF-β controlled MSC expressing IL-12 or nCD47-SLAMF7, MSC-IL-12 or MSC-nCD47-SLAMF7 were cultured in MSC complete media in the presence or absence of TGF-β1 (Abcam) and/or TGF-β2 (Abcam) at a concentration of 10 ng/ml. IL-12 or nCD47-SLAMF7 expression was assessed by Western blot and ELISA (biolegend). Viral vector was packaged from HEK293 cells.

In Vitro Cellular expression and target ability of IL-12 or nCD47-SLAMF7

To determine which MSCs responded to TGFβ and expressed IL-12 or nCD47-SLAMF7, as well as to examine the cellular co-localization of IL-12 and nCD47-SLAMF7 in the culture medium, GL261 cells, MSC-IL-12, MSC-nCD47-SLAMF7, and CD8 T cells from mouse spleen were seeded in

glass-bottom cell culture dishes (NEST, catalog no. 801001; 1×10^5 cells per well). They were then incubated with a culture medium containing TGFβ or medium obtained from MSC-IL-12 or MSC-nCD47-SLAMF7 for 3 hours. Subsequently, these cells were washed three times with PBS, fixed in 1% paraformaldehyde for 15 minutes, and then washed with PBS again. Cellular imaging was performed using confocal laser scanning microscopy (LSM 710). For quantitative assessment of cellular uptake, cells were seeded in six-well cell culture dishes and treated as described above. They were then washed with PBS three times, collected, fixed, and resuspended in PBS for flow cytometry detection.

Native SDS-PAGE to Verify the IL-12 and nCD47-SLAMF7

The procedure was similar to conventional SDS-PAGE, with the exception that the gel and electrophoresis buffers did not contain SDS. We mixed 5× loading buffer with culture medium obtained from MSC-IL-12 or MSC-nCD47-SLAMF7 and then added the electrophoretic sample to the gel. Finally, the PAGE gel was stained with Coomassie Brilliant Blue solution.

Western Blotting

The cell culture medium was treated with RIPA lysis buffer, and protein separation was carried out on an 8% SDS-PAGE gel. Subsequently, membrane transfer was performed using a 0.2 μm PVDF membrane (Millipore), followed by antibody incubation. The IL-12 antibody (Catalog number: 17645-1-AP), SLAMF7 antibody (Catalog number: 12905-1-AP), and β-actin antibody (Catalog number: 81115-1-RR) were all purchased from Proteintech. All images were acquired using the ChemiDoc Imaging System (Bio-Rad).

Horizontal chemotactic mobility assay

The experimental design was adapted from the IBIDITM Culture-Inserts system, which employs two chambers to separate different cell types on opposite sides[38]. For in vitro real-time chemotactic mobility assays, the culture inserts were transferred to a 35 mm diameter petri dish. The astrocyte culture medium and the GL261 culture medium were seeded in each well of the culture inserts, with a volume of 1 mL per

well. After incubation for 1 day, the Culture-Inserts were removed, creating a 500 μm cell-free gap. The cell culture dish was placed in an incubator providing a constant temperature of 37°C and 5% CO2 for 24 hours. Subsequently, the cells were fixed with 4% paraformaldehyde and observed using an inverted fluorescence microscope (Zeiss, Oberkochen, Germany).

Animal Model Experiments and Evaluation of Therapeutic Effects

To establish the GBM model, mice were anesthetized with a 1% pentobarbital sodium solution before all surgical procedures. GL261-luciferase (LUC) cells (1×106 cells suspended in 10 μL of PBS) were stereotactically injected into the right ventricle's striatum. Four days after the inoculation with GL261-luciferase cells, each mouse underwent bioluminescence imaging to ensure the successful and uniform establishment of the GBM model. Subsequently, the mice were randomly divided into five groups: PBS, MSC, MSC-IL-12, MSC-nCD47-SLAMF7, and MSC-IL-12/MSC-nCD47-SLAMF7 and were given their respective treatments. To assess the development of the GBM model, six mice in each group were imaged on the day when all treatments were completed under 1% pentobarbital sodium anesthesia using the Bruker In Vivo MS FX PRO Imager.

Bioluminescence Imaging

After anesthetizing C57 mice with 1% pentobarbital sodium, they were intraperitoneally injected with firefly luciferin (150 mg kg−1; Sigma-Aldrich; CAS: 103404-75-7). After 15 minutes, mice were imaged using the Bruker In Vivo MS FX PRO Imager with 3-minute exposure times for acquiring luminescent images.

Tissue Multicolor Immunofluorescent Staining

Tissue multicolor immunofluorescent staining was performed using the OpalTM 7-Color Manual IHC Kit (NEL811001KT, PerkinElmer). Tumor tissues were fixed, embedded in paraffin, and sectioned with a microtome. The sections were then dewaxed and hydrated routinely. Antigen retrieval was achieved by applying a Tris-EDTA Buffer solution, and endogenous peroxidases were quenched using 3% H2O2. Samples were subsequently blocked with normal goat serum. The slides were incubated overnight with the following antibodies: Alexa Fluor® 647 anti-mouse

CD206 (MMR) Antibody (Biolegend, cat# 141711), Alexa Fluor® 594 anti-mouse F4/80 Antibody (Biolegend, cat# 123140), PE anti-mouse CD319 Antibody (Biolegend, cat# 152005), Alexa Fluor 594® anti-mouse CD172a Antibody (Biolegend, cat# 144020), and Alexa Fluor® 647 anti-mouse CD47 Antibody (Biolegend, cat# 127509). Subsequently, DAPI was applied for 20 minutes at room temperature. Finally, tissue immunofluorescence was analyzed using the PE Vectra (PerkinElmer).

Collection of Tumor-Infiltrating Immunocytes

Tumor-infiltrating immune cells were obtained from GBM model as previously described[39].

Flow cytometry

For cell-surface analysis, cells were stained with the anti-mouse Zombie NIR Fixable Viability Kit (423106) and incubated with antibodies against CD45 (103114), CD11b (101205), F4/80 (123121), CD3 (100212), CD4 (100408), and CD8a (100752) at the recommended concentrations. Incubation was carried out at 4 °C for 30 minutes. For T-cell intracellular IFN-γ (505808) cytokine staining, cells were fixed and permeabilized after stimulation with Phorbol 12-myristate 13-acetate (PMA) (ab120297, Abcam, 100 ng mL−1), Monensin sodium salt (ab120499, Abcam, 1 ug mL−1), and Ionomycin calcium salt (5608212, PeproTech, 100 ng mL−1) for 3 hours.For CD206 (141706) and TCF-1 (655203) staining, cells were also fixed and permeabilized. All flow cytometry antibodies were purchased from Biolegend (San Diego, CA, USA).

Cytokine Detection

The supernatant from mouse GBM model tissue fragmentation was collected for cytokine detection. The LEGENDplex Mouse Cytokine Release Syndrome Panel (13-plex) with VBottom Plate (purchased from Biolegend)

Statistical Analysis

The unpaired two-tailed Student's t-test to compare the differences between the two groups was used, while survival rates were evaluated with the log-rank Mantel-Cox test using GraphPad Prism 7 software. Repeated measurements of tumor volume

growth were compared using One-way analysis of variance (ANOVA). Flow cytometry data were analyzed using FlowJo.10. Significant differences between the groups are indicated by *p < 0.05, **p < 0.01, and ***p < 0.001, and NS, not significant.

Data availability

The authors declare that all data supporting the results of this study are available in the paper and supplementary information. Source data are provided in this paper.

Acknowledgments

This research was supported by the National Natural Science Foundation of China (No. 81502174, No. 82001193).

Competing interests

The authors declare no competing interest.

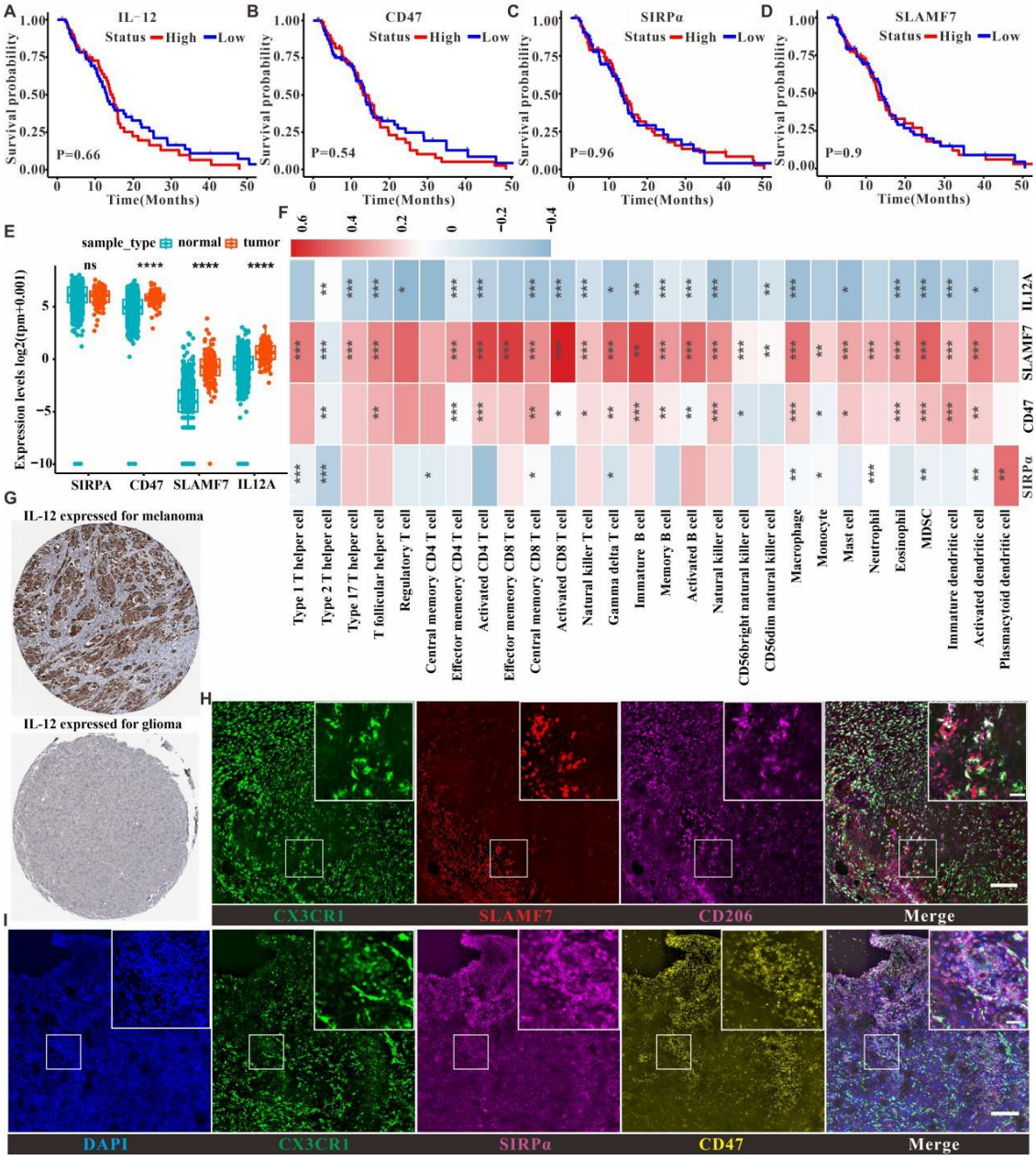

Figure 1. Identification of clinical correlations between different functional proteins and glioma patients. (A) Correlation of IL-12 with prognostic survival of clinical patients. (B) Correlation of CD47 with prognostic survival of clinical patients. (C) Correlation of SIRPα with prognostic survival of clinical patients. (D) Correlation of SLAMF7 with prognostic survival of clinical patients. (E) Relationship of the expression of different functional proteins in tumors and adjacent cancer. (F) Correlation of different functional proteins with different immune cell infiltration in clinical samples correlation. (G) HPA database-based analysis of IL-12 expression in melanoma and glioma patients. (H) Immunofluorescence analysis of SLAMF7 expression in mouse glioma microenvironment, scale bar is 100 μm in the unenlarged figure and 20 μm in the enlarged small figure; (I) Immunofluorescence analysis of

CD47 and SIRPα expression in mouse glioma microenvironment, scale bar is the same as that of Figure H.

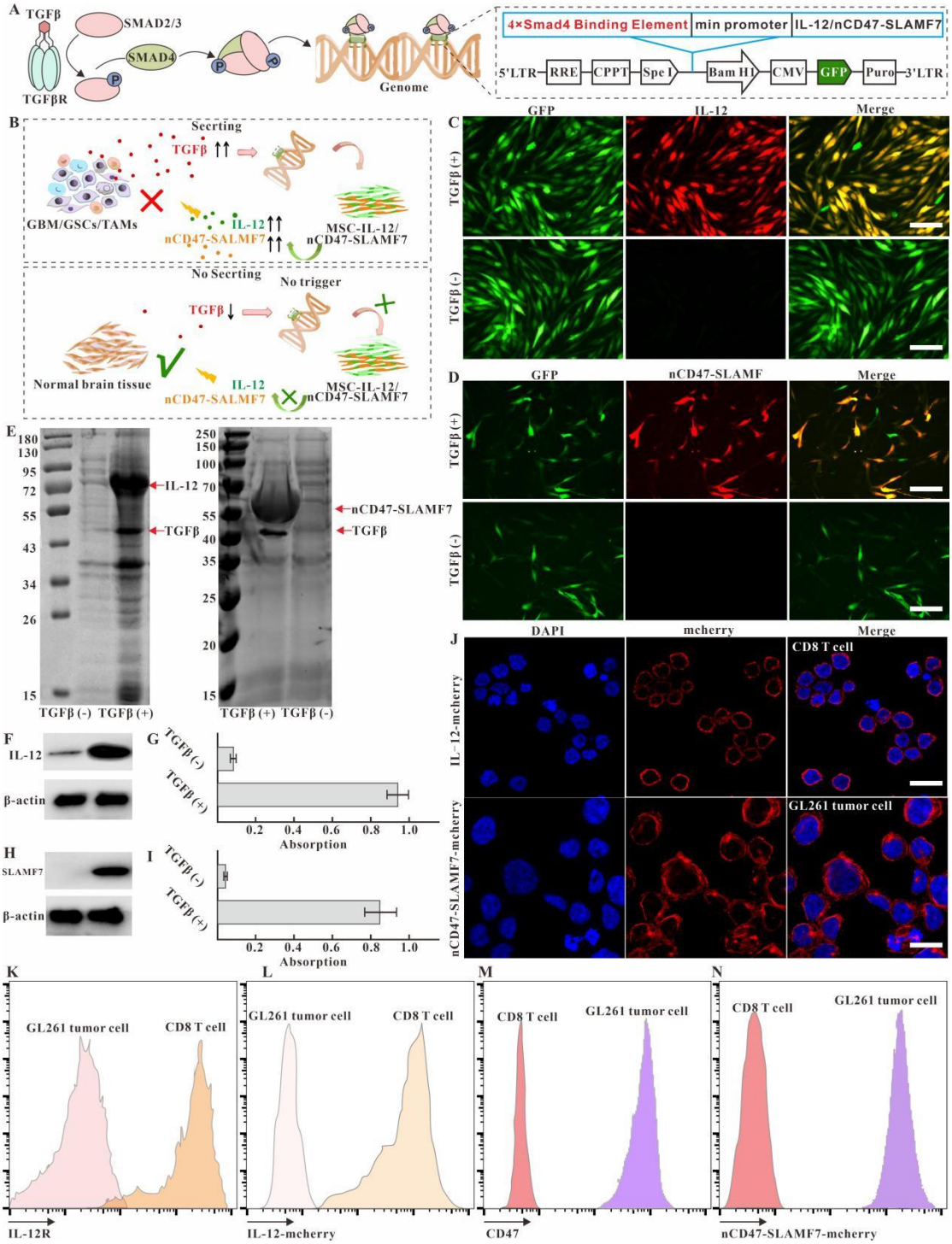

Figure 2. Validation of controlled expression, structural accuracy, and targeting of IL-12 or nCD47-SLAMF7 to immune cells in MSC culture medium. (A) Schematic diagram related to the gene regulatory mechanism of MSC releasing IL-12 or nCD47-SLAMF7 in response to TGFβ cytokines. (B) Schematic diagram of the mechanism of MSC releasing IL-12 or nCD47-SLAMF7 in response to tumor supernatant. (C) Confocal imaging identifies that MSC-IL-12 can express IL-12 cytokines in response to TGFβ. The scale bar is 50 μm. (D) Confocal imaging

identifies that MSC-nCD47-SLAMF7 expresses nCD47-SLAMF7 fusion proteins in response to TGFβ. The scale bar is 20 μm. (E) Relative molecular weights of IL-12 and nCD47-SLAMF7 secreted by MSC were identified by non-denaturing SDS-PAGE gels. (F) Western blotting identification of IL-12 expression. (G) Elisa's identification of IL-12 in MSC supernatants. (H) Western blotting identification of nCD47-SLAMF7 expression. (I) Elisa identification of nCD47-SLAMF7 in MSC supernatants. (J) Confocal imaging identification of IL -12 or nCD47-SLAMF7 ability to target T cells or GL261 tumor cells. (K) Flow cytometry identification of IL-12 receptor expression in CD8 T cells. (L) Flow cytometry identification of IL-12 cytokine targeting ability to CD8 T cells. (M) Flow cytometry identification of CD47 molecule expression in GL261 cells. (N) Flow cytometry characterization of the targeting ability of nCD47-SLAMF7 on GL261 cells.

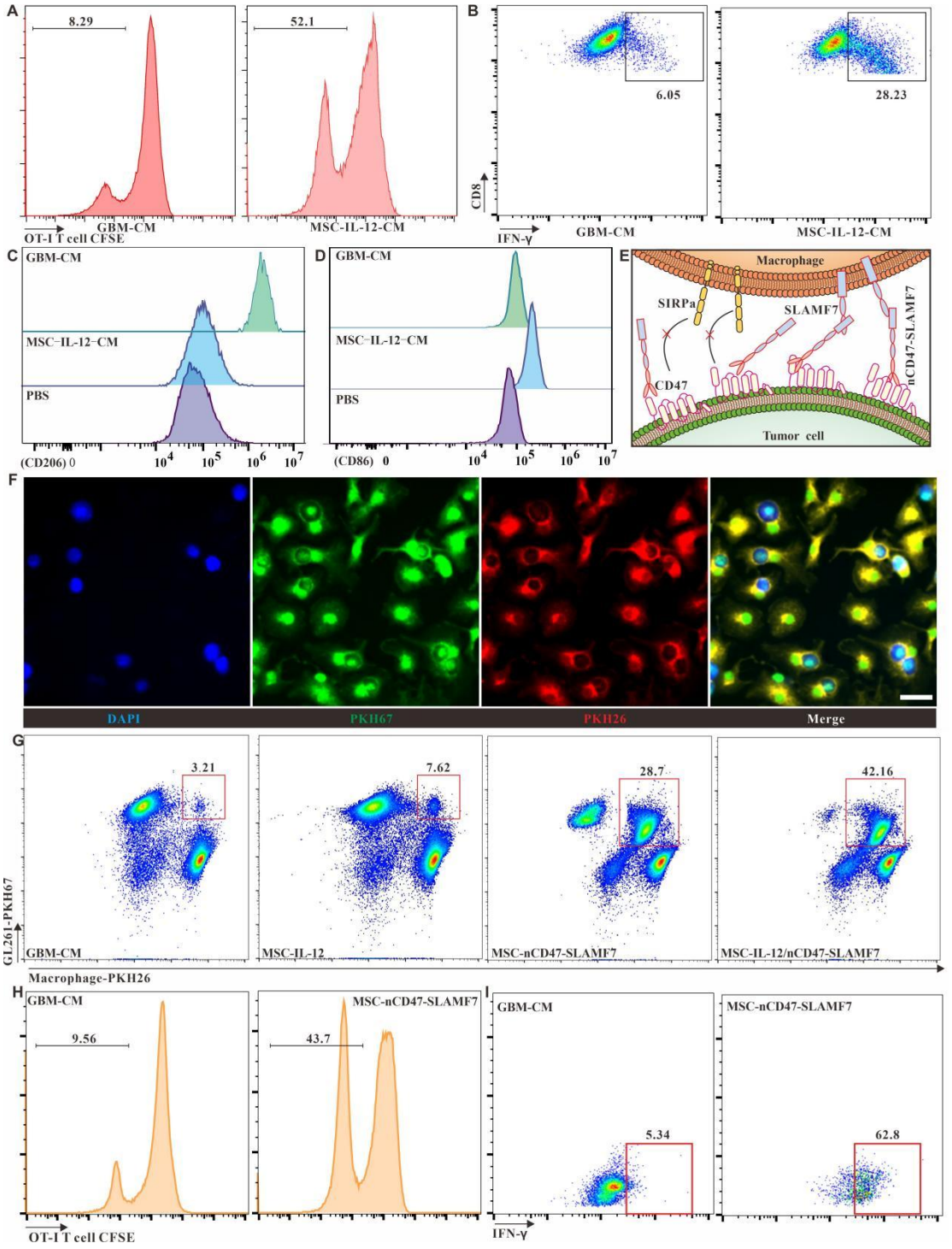

Figure 3. Assessment of the functional impact of IL-12 or nCD47-SLAMF7 in MSC supernatants on CD8 T cells and macrophages. (A) Flow cytometric analysis of the proliferation of CD8 T cells in response to GBM-derived versus MSC-IL-12-derived supernatants. (B) Analysis of CD8 T cell activation and IFN-γ release when cultured with GBM-derived or MSC-IL-12-derived supernatants. (C) Determination of CD206 expression on bone marrow-derived M0 macrophages exposed to GBM-derived or MSC-IL-12 supernatants. (D) Examination of CD86 molecule expression on M0 macrophages in response to different supernatants. (E) Illustration of how nCD47-SLAMF7 fusion proteins influence macrophage phagocytosis of tumor cells.

(F) Confocal microscopy to evaluate the enhancement of glioma cell phagocytosis by macrophages due to MSC-nCD47-SLAMF7 supernatants, with a scale bar of 20 μm. (G) Comparative flow cytometry to assess the promotion of tumor cell uptake by macrophages using supernatants from various cellular sources. (H) Investigation of OT-I T cell proliferation induced by macrophages that have phagocytosed GL261-OVA$^{\beta 2m-/-}$ cells. (I) Analysis of cytokine secretion, such as IFN-γ, by OT-I T cells in response to macrophages with internalized GL261-OVA$^{\beta 2m-/-}$ cells.

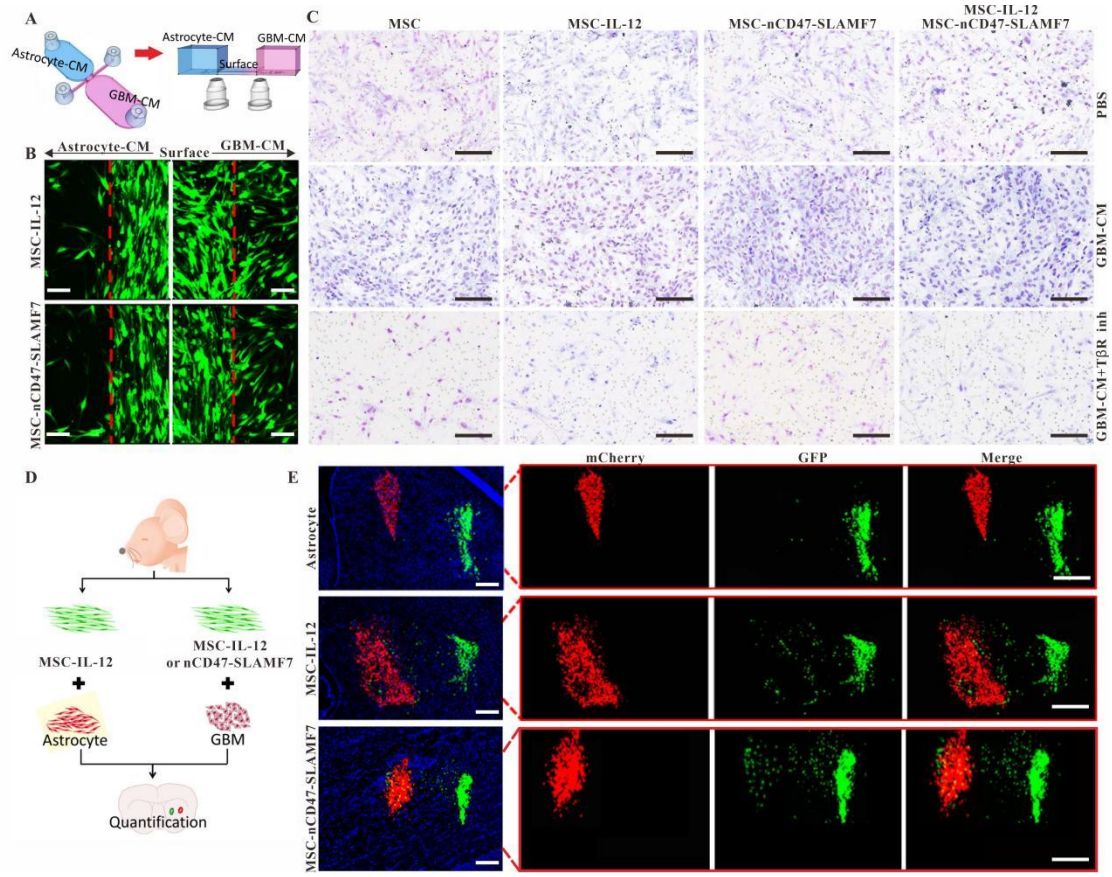

Figure 4. Evaluation of the tumor-homing capabilities of MSC-IL-12 and MSC-nCD47-SLAMF7. (A) Illustrative schematic of the personalized Transwell model design. (B) Confocal microscopy shows MSC-IL-12 and MSC-nCD47-SLAMF7 migrating towards a GBM-derived supernatant, with a scale bar representing 50 μm. (C) H&E staining demonstrates the homing of MSC-IL-12 and MSC-nCD47-SLAMF7 in response to a GBM supernatant with or without TGFβ or TGFβ receptor inhibitors; scale bar is 100 μm. (D) Conceptual schematic of the in vivo study designed to validate the tumor-homing efficiency of MSC-IL-12 and MSC-nCD47-SLAMF7. (E) Confocal microscopy characterizes the in vivo tumor-homing of MSC-IL-12 and MSC-nCD47-SLAMF7, indicated by a scale bar of 100 μm.

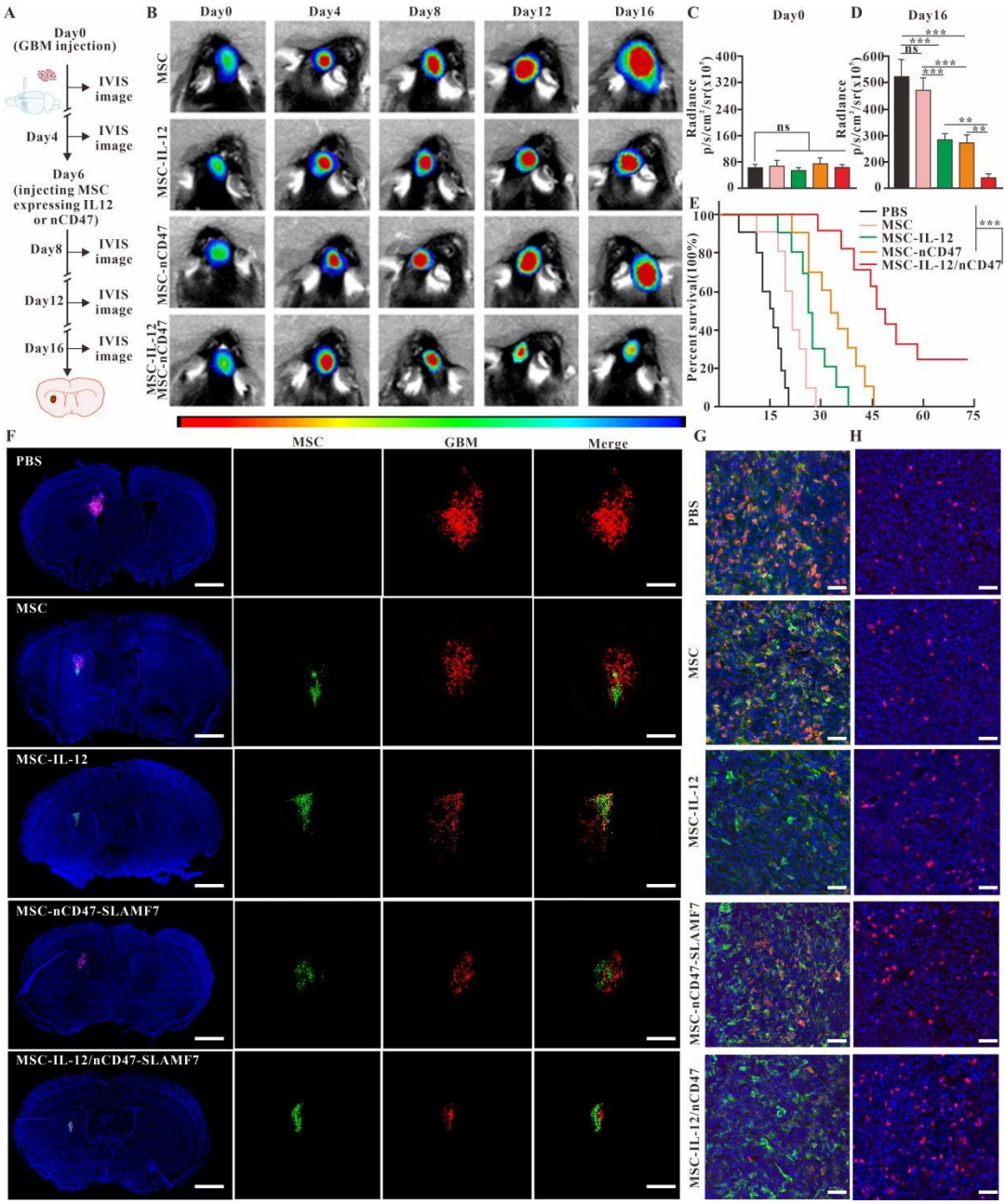

Figure 5. In vitro validation of the therapeutic potential of MSC-IL-12 and MSC-nCD47-SLAMF7 against glioma. (A) Diagram illustrating the treatment process using MSCs engineered to express various functional proteins. (B) Live imaging of small animals to track glioma progression in different treatment groups over time. (C) Measurement of glioma bioluminescence intensity in various treatment groups on day 0. (D) Measurement of glioma bioluminescence intensity in various treatment groups on day 16. (E) Analysis of the survival rates in the GL261 in situ mouse model. (F) Immunofluorescence to visualize the localization of MSCs expressing distinct functional proteins at the glioma site. Scale bar: 1 mm (left panel), 200 μm (right panel). (G) Immunofluorescence to demonstrate macrophage CD206 expression across different treatment groups. Scale bar: 50 μm. (H) Immunofluorescence to assess CD8 T cell infiltration in the various treatment groups. Scale bar: 50 μm.

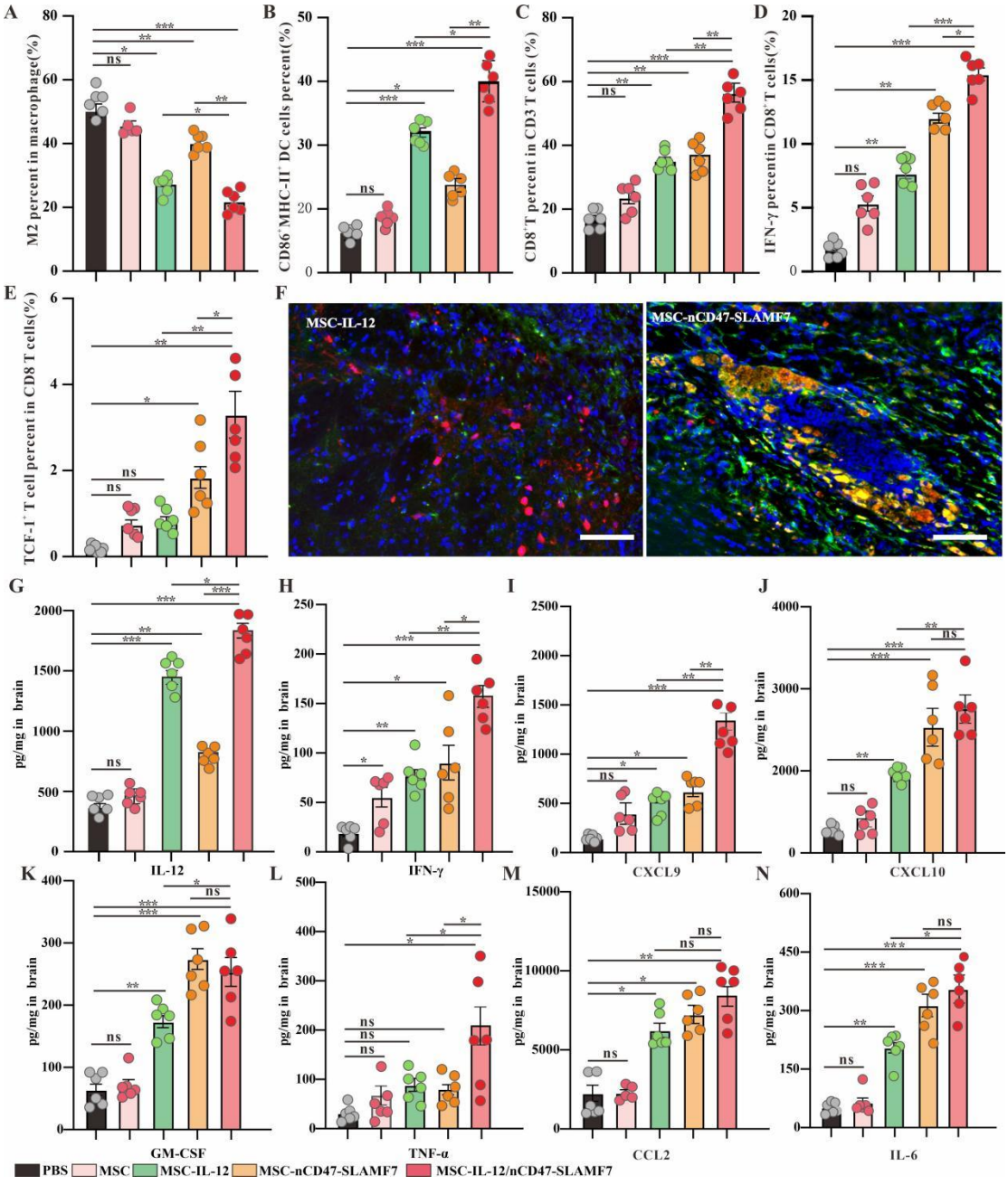

Figure 6. Validation of the ability of MSC-IL-12 and MSC-nCD47-SLAMF7 to reverse the TIME. (A) Identification of the proportion of M2-type macrophages in different given treatment groups. (B) Identification of the proportion of mature DC cells in different given treatment groups. (C) Identification of the proportion of CD8 T cells occupying CD3 T cells in different given treatment groups. (D) Identification of the proportion of IFN-γ-positive CD8 T cells in different given treatment groups. (E) Identification of the proportion of exhausted precursor CD8 T cells in different given treatment groups. (F) Immunofluorescence to identify that in vivo injection of MSC-nCD47-SLAMF7 promotes the uptake of tumor cells by macrophages, with a scale bar of 100 μm. (G) Identification of IL-12 content in the lysed supernatant of the mouse brain in different given treatment groups. (H) Identification of IFN-γ content in the lysed supernatant of the mouse brain in different given treatment groups. (I)

Determination of CXCL9 in mouse brain lysate supernatant in different given treatment groups. (J) Determination of CXCL10 in mouse brain lysate supernatant in different given treatment groups. (K) Determination of GM-CSF in mouse brain lysate supernatant in different given treatment groups. (L) Determination of TNF-α in mouse brain lysate supernatant in different given treatment groups. (M) Determination of CCL2 in the lysed supernatant of mouse brain in different given treatment groups. (N) Determination of IL-6 in the lysed supernatant of mouse brain in different given treatment groups.

Reference

1.Lapointe, S., Perry, A. & Butowski, N.A. Primary brain tumours in adults. Lancet 392, 432-446 (2018).

2.Sampson, J.H., Gunn, M.D., Fecci, P.E. & Ashley, D.M. Brain immunology and immunotherapy in brain tumours. Nature reviews. Cancer 20, 12-25 (2020).

3. Morad, G., Helmink, B.A., Sharma, P. & Wargo, J.A. Hallmarks of response, resistance, and toxicity to immune checkpoint blockade. Cell 185, 576 (2022).

4. Quail, D.F. & Joyce, J.A. The Microenvironmental Landscape of Brain Tumors. Cancer cell 31, 326-341 (2017).

5. He, L. et al. Wnt/β-catenin signaling cascade: A promising target for glioma therapy. Journal of cellular physiology 234, 2217-2228 (2019).

6. Ding, X.C. et al. The relationship between expression of PD-L1 and HIF-1α in glioma cells under hypoxia. Journal of hematology & oncology 14, 92 (2021).

7. Zhai, L. et al. Immunosuppressive IDO in Cancer: Mechanisms of Action, Animal Models, and Targeting Strategies. Frontiers in immunology 11, 1185 (2020).

8. Qiu, J. et al. Small-molecule inhibition of prostaglandin E receptor 2 impairs cyclooxygenase-associated malignant glioma growth. British journal of pharmacology 176, 1680-1699 (2019).

9. Mi, Y. et al. The Emerging Role of Myeloid-Derived Suppressor Cells in the Glioma Immune Suppressive Microenvironment. Frontiers in immunology 11, 737 (2020).

10. Kadiyala, P. et al. Inhibition of 2-hydroxyglutarate elicits metabolic reprogramming and mutant IDH1 glioma immunity in mice. The Journal of clinical investigation 131 (2021).

11. Christofides, A. et al. The complex role of tumor-infiltrating macrophages. Nature immunology 23, 1148-1156 (2022).

12. Zhang, W. et al. Advances in Anti-Tumor Treatments Targeting the CD47/SIRPα Axis. Frontiers in immunology 11, 18 (2020).

13. Jiang, N. et al. Fatty acid oxidation fuels glioblastoma radioresistance with CD47-mediated immune evasion. Nature communications 13, 1511 (2022).

14. Tang, Z. et al. CD47 masks pro-phagocytic ligands in cis on tumor cells to suppress antitumor immunity. Nature immunology 24, 2032-2041 (2023).

15. Jiang, Z., Sun, H., Yu, J., Tian, W. & Song, Y. Targeting CD47 for cancer immunotherapy. Journal of hematology & oncology 14, 180 (2021).

16. Lu, Y. et al. Immunological conversion of solid tumours using a bispecific nanobioconjugate for cancer immunotherapy. Nature nanotechnology 17, 1332-1341 (2022).

17. Zhao, Y. & Zhou, X. Engineering chimeric antigen receptor-natural killer cells for cancer immunotherapy. Immunotherapy 12, 653-664 (2020).

18. Chen, Y. et al. CAR-macrophage: A new immunotherapy candidate against solid tumors. Biomedicine & pharmacotherapy = Biomedecine & pharmacotherapie 139, 111605 (2021).

19. Dolton, G. et al. Targeting of multiple tumor-associated antigens by individual T cell receptors during successful cancer immunotherapy. Cell 186, 3333-3349.e3327 (2023).

20.Ma, L. et al. Vaccine-boosted CAR T crosstalk with host immunity to reject tumors with antigen heterogeneity. Cell 186, 3148-3165.e3120 (2023).

21.Yarmarkovich, M. et al. Cross-HLA targeting of intracellular oncoproteins with peptide-centric CARs. Nature 599, 477-484 (2021).

22. O'Rourke, D.M. et al. A single dose of peripherally infused EGFRvIII-directed CAR T cells mediates antigen loss and induces adaptive resistance in patients with recurrent glioblastoma. Science translational medicine 9 (2017).

23. Pittenger, M.F. et al. Mesenchymal stem cell perspective: cell biology to clinical progress. NPJ Regenerative medicine 4, 22 (2019).

24. Andrzejewska, A., Dabrowska, S., Lukomska, B. & Janowski, M. Mesenchymal Stem Cells for Neurological Disorders. Advanced science 8, 2002944 (2021).

25. Bhere, D. et al. Target receptor identification and subsequent treatment of resected brain tumors with encapsulated and engineered allogeneic stem cells. Nature communications 13, 2810 (2022).

26. Weng, Z. et al. Therapeutic roles of mesenchymal stem cell-derived extracellular vesicles in cancer. Journal of hematology & oncology 14, 136 (2021).

27. Kimbrel, E.A. & Lanza, R. Next-generation stem cells - ushering in a new era of cell-based therapies. Nature reviews. Drug discovery 19, 463-479 (2020).

28. Vicinanza, C. et al. Modified mesenchymal stem cells in cancer therapy: A smart weapon requiring upgrades for wider clinical applications. World journal of stem cells 14, 54-75 (2022).

29. Li, M. et al. Transforming Growth Factor-β Promotes Homing and Therapeutic Efficacy of Human Mesenchymal Stem Cells to Glioblastoma. Journal of neuropathology and experimental neurology 78, 315-325 (2019).

30. Li, M. et al. Exploiting tumor-intrinsic signals to induce mesenchymal stem cell-mediated suicide gene therapy to fight malignant glioma. Stem cell research & therapy 10, 88 (2019).

31. Gutierrez, E. et al. An optimized IL-12-Fc expands its therapeutic window, achieving strong activity against mouse tumors at tolerable drug doses. Med (New York, N.Y.) 4, 326-340.e325 (2023).

32. Agarwal, Y. et al. Intratumourally injected alum-tethered cytokines elicit potent and safer local and systemic anticancer immunity. Nature biomedical engineering 6, 129-143 (2022).

33. Chowdhury, S., Castro, S., Coker, C., Hinchliffe, T.E. & Arpaia, N. Programmable bacteria induce durable tumor regression and systemic antitumor immunity. 25, 1057-1063 (2019).

34. Chen, J. et al. SLAMF7 is critical for phagocytosis of haematopoietic tumour cells via Mac-1 integrin. Nature 544, 493-497 (2017).

35. Huang, C. et al. Sirpalpha on tumor-associated myeloid cells restrains antitumor immunity in colorectal cancer independent of its interaction with CD47. Nature cancer (2024).

36. Lo, B.C. et al. Microbiota-dependent activation of CD4(+) T cells induces CTLA-4 blockade-associated colitis via Fcgamma receptors. Science 383, 62-70 (2024).

37. Dai, X. et al. USP7 targeting modulates anti-tumor immune response by reprogramming Tumor-associated Macrophages in Lung Cancer. Theranostics 10, 9332-9347 (2020).
38. Shih, Y.T. et al. Modulation of chemotactic and pro-inflammatory activities of endothelial progenitor cells by hepatocellular carcinoma. Cellular signalling 24, 779-793 (2012).
39. Lu, L. et al. Targeted immunomodulation of inflammatory monocytes across the blood-brain barrier by curcumin-loaded nanoparticles delays the progression of experimental autoimmune encephalomyelitis. Biomaterials 245, 119987 (2020).

Supporting information

Table1. the protein sequence used in the study.

Protein name	Peptide sequence
IL-12 (P35-P2A-P40)	MCQSRYLLFLATLALLNHLSLARVIPVSGPARCLSQSRNLLKTT DDMVKTAREKLKHYSCTAEDIDHEDITRDQTSTLKTCLPLELHK NESCLATRETSSTTRGSCLPPQKTSLMMTLCLGSIYEDLKMYQT EFQAINAALQNHNHQQIILDKGMLVAIDELMQSLNHNGETLRQ KPPVGEADPYRVKMKLCILLHAFSTRVVTINRVMGYLSSAGSGA TNFSLLKQAGDVEENPGPGSGMCPQKLTISWFAIVLLVSPLMAM WELEKDVYVVEVDWTPDAPGETVNLTCDTPEEDDITWTSDQR HGVIGSGKTLTITVKEFLDAGQYTCHKGGETLSHSHLLLHKKEN GIWSTEILKNFKNKTFLKCEAPNYSGRFTCSWLVQRNMDLKFNI KSSSSSPDSRAVTCGMASLSAEKVTLDQRDYEKYSVSCQEDVT CPTAEETLPIELALEARQQNKYENYSTSFFIRDIIKPDPPKNLQM KPLKNSQVEVSWEYPDSWSTPHSYFSLKFFVRIQRKKEKMKET EEGCNQKGAFLVEKTSTEVQCKGGNVCVQAQDRYYNSSCSKW ACVPCRVRS
Mcherry	MVSKGEEDNMAIIKEFMRFKVHMEGSVNGHEFEIEGEGEGRPY EGTQTAKLKVTKGGPLPFAWDILSPQFMYGSKAYVKHPADIPD YLKLSFPEGFKWERVMNFEDGGVVTVTQDSSLQDGEFIYKVKL RGTNFPSDGPVMQKKTMGWEASSERMYPEDGALKGEIKQRLK LKDGGHYDAEVKTTYKAKKPVQLPGAYNVNIKLDITSHNEDYT IVEQYERAEGRHSTGGMDELYK
IL-12- mcherry	MCQSRYLLFLATLALLNHLSLARVIPVSGPARCLSQSRNLLKTT DDMVKTAREKLKHYSCTAEDIDHEDITRDQTSTLKTCLPLELHK NESCLATRETSSTTRGSCLPPQKTSLMMTLCLGSIYEDLKMYQT EFQAINAALQNHNHQQIILDKGMLVAIDELMQSLNHNGETLRQ KPPVGEADPYRVKMKLCILLHAFSTRVVTINRVMGYLSSAGSGA TNFSLLKQAGDVEENPGPGSGMCPQKLTISWFAIVLLVSPLMAM WELEKDVYVVEVDWTPDAPGETVNLTCDTPEEDDITWTSDQR HGVIGSGKTLTITVKEFLDAGQYTCHKGGETLSHSHLLLHKKEN GIWSTEILKNFKNKTFLKCEAPNYSGRFTCSWLVQRNMDLKFNI KSSSSSPDSRAVTCGMASLSAEKVTLDQRDYEKYSVSCQEDVT CPTAEETLPIELALEARQQNKYENYSTSFFIRDIIKPDPPKNLQM KPLKNSQVEVSWEYPDSWSTPHSYFSLKFFVRIQRKKEKMKET EEGCNQKGAFLVEKTSTEVQCKGGNVCVQAQDRYYNSSCSKW ACVPCRVRSGGGGSGGGGSGGGGSGGGGSMVSKGEEDNMAII KEFMRFKVHMEGSVNGHEFEIEGEGEGRPYEGTQTAKLKVTKG GPLPFAWDILSPQFMYGSKAYVKHPADIPDYLKLSFPEGFKWER VMNFEDGGVVTVTQDSSLQDGEFIYKVKLRGTNFPSDGPVMQ KKTMGWEASSERMYPEDGALKGEIKQRLKLKDGGHYDAEVK TTYKAKKPVQLPGAYNVNIKLDITSHNEDYTIVEQYERAEGRHS TGGMDELYK
CD47 nanobody	DIVMTQSPATLSVTPGDRVSLSCRASQTISDYLHWYQQKSHESP

(VL-Linker-VH)	RLLIKFASQSISGIPSRFSGSGSGSDFTLSINSVEPEDVGVYYCQN GHGFPRTFGGGTKLEIKGGGGSGGGGSGGGGSGGGGSEVQLVE SGGDLVKPGGSLKLSCAASGFTFSGYGMSWVRQTPDKRLEWV ATITSGGTYTYYPDSVKGRFTISRDNAKNTLYLQIDSLKSEDTAI YFCARSLAGNAMDYWGQGTSVTVSS
SLAMF7$_{23-224}$	SGTLKKVAGALDGSVTFTLNITEIKVDYVVWTFNTFFLAMVKK DGVTSQSSNKERIVFPDGLYSMKLSQLKKNDSGAYRAEIYSTSS QAS LIQEYVLHVY KHLSRPKVTI DRQSNKNGTCVINLTCSTDQ DGENVTYSWKAVGQGDNQFHDGATLSIAWRSGEKDQALTCMA RNPVSNSFSTPVFPQKLC EDAATDLTSLRG
nCD47-SLAMF7	MASPLTRFLSLNLLLLGESIILGSGEADIVMTQSPATLSVTP GDRVSLSCRASQTISDYLHWYQQKSHESPRLLIKFASQSISGIPSR FSGSGSGSDFTLSINSVEPEDVGVYYCQNGHGFPRTFGGGTKLEI KGGGGSGGGGSGGGGSGGGGSEVQLVESGGDLVKPGGSLKLS CAASGFTFSGYGMSWVRQTPDKRLEWVATITSGGTYTYYPDSV KGRFTISRDNAKNTLYLQIDSLKSEDTAIYFCARSLAGNAMDY WGQGTSVTVSSGGGSGGGGGGSGGGGSGTLKKVAGALD GSVTFTLNITEIKVDYVVWTFNTFFLAMVKKDGVTSQSSNKERI VFPDGLYSMKLSQLKKNDSGAYRAEIYSTSSQASLIQEYVLHVY KHLSRPKVTIDRQSNKNGTCVINLTCSTDQDGENVTYSWKAVG QGDNQFHDGATLSIAWRSGEKDQALTCMARNPVSNSFSTPVFP QKLC EDAATDLTSLRG
nCD47-SLAMF7-mcherry	MASPLTRFLSLNLLLLGESIILGSGEADIVMTQSPATLSVTP GDRVSLSCRASQTISDYLHWYQQKSHESPRLLIKFASQSISGIPSR FSGSGSGSDFTLSINSVEPEDVGVYYCQNGHGFPRTFGGGTKLEI KGGGGSGGGGSGGGGSGGGGSEVQLVESGGDLVKPGGSLKLS CAASGFTFSGYGMSWVRQTPDKRLEWVATITSGGTYTYYPDSV KGRFTISRDNAKNTLYLQIDSLKSEDTAIYFCARSLAGNAMDY WGQGTSVTVSSGGGSGGGGGGSGGGGSGTLKKVAGALD GSVTFTLNITEIKVDYVVWTFNTFFLAMVKKDGVTSQSSNKERI VFPDGLYSMKLSQLKKNDSGAYRAEIYSTSSQASLIQEYVLHVY KHLSRPKVTIDRQSNKNGTCVINLTCSTDQDGENVTYSWKAVG QGDNQFHDGATLSIAWRSGEKDQALTCMARNPVSNSFSTPVFP QKLCEDAATDLTSLRGGGGGSGGGGSGGGGSGGGGSMVSKGE EDNMAIIKEFMRFKVHMEGSVNGHEFEIEGEGEGRPYEGTQTA KLKVTKGGPLPFAWDILSPQFMYGSKAYVKHPADIPDYLKLSFP EGFKWERVMNFEDGGVVTVTQDSSLQDGEFIYKVKLRGTNFPS DGPVMQKKTMGWEASSERMYPEDGALKGEIKQRLKLKDGGH YDAEVKTTYKAKKPVQLPGAYNVNIKLDITSHNEDYTIVEQYE RAEGRHSTGGMDELYK